Multiscale Domain Decomposition Preconditioners for Anisotropic High-Contrast Problems

Yalchin Efendiev[1], Juan Galvis[1], Raytcho Lazarov[1], Svetozar Margenov[2], and Jun Ren[1]

[1] Department of Mathematics, TAMU, College Station, TX 77843-3368, USA.
[2] Acad. G. Bonchev Str., bl. 25A, Institute of Information and Communication Technologies, Bulgarian Academy of Sciences, Sofia 1113, BULGARIA.

1 Summary

In this paper, we study robust two-level domain decomposition preconditioners for highly anisotropic multiscale problems. We present a construction of coarse spaces that emploies initial multiscale basis functions and discuss techniques to achieve smaller dimensional coarse spaces without sacrificing the robustness of the preconditioner. We also present numerical results and consider possible extensions of these approaches where the dimension of the coarse space can be reduced further.

2 Introduction

Anisotropy in the diffusion arises in many applications in geosciences and engineering. In flows porous media, high anisotropy can be due to the presence of fractures that may have preferred high-conductivity directions. Because of high variations among the matrix and fracture conductivities, the permeability can have high anisotropy at the fine-scale. This is the case when fracture network conducts only in some preferred directions (e.g., in one direction in 2D problems and one or two directions in 3D problems). This preferred direction is the direction of high anisotropy and it can have heterogeneous spatial variations. For example, the presence of fracture pockets can create highly anisotropic isolated regions, while fracture corridors can form long highly anisotropic channels that span a rich hierarchy of scales. It is a challenging task to design robust preconditioners for such problems (e.g., [4]) or to solve them on a coarse grid (e.g., [2]).

In this paper, we discuss robust preconditioners for highly anisotropic multiscale diffusion problems. We assume that the high-anisotropy is also highly heterogeneous over the problem domain and these spatial variations cannot be captured within a coarse block. In the paper, robust two-level domain decomposition preconditioners are constructed by designing coarse spaces that contain essential features of the fine-scale solution. The construction of the coarse spaces is based on recently introduced

R. Bank et al. (eds.), *Domain Decomposition Methods in Science and Engineering XX*, Lecture Notes in Computational Science and Engineering 91,
DOI 10.1007/978-3-642-35275-1_33, © Springer-Verlag Berlin Heidelberg 2013

methods [1, 3]. We show that, for anisotropic problems, the coarse spaces can have a large dimension because fine-scale features within high-anisotropy regions need to be represented on a coarse grid. In this paper, we propose a number of remedies for this problem. Note that the proposed methods differ from existing methods for anisotropic problems [4].

The coarse spaces used in two-level domain decomposition preconditioners are constructed based on local spectral problems with a pre-computed scalar weight function. The computation of the weight function uses an initial coarse space where one basis function per coarse node is defined. We show that the local eigenvalue problem can contain many small eigenvalues, which are asymptotically vanishing as the contrast increases. One needs to include all eigenvectors that correspond to these small, asymptotically vanishing, eigenvalues. Because the number of these small eigenvalues defines the dimension of the coarse space, it is important to choose a weight function such that the dimension of the coarse space is as small as possible. If we consider the initial space as the span of piecewise (bi)linear functions, then the dimension of the coarse space can be very large. In particular, the coarse space contains all fine-scale functions with respect to the slow variable (defined as the variable representing the direction of slow conductivity) within high-anisotropy regions. On the other hand, using multiscale basis functions [2] in the initial space allows capturing the effects of high-conductivity inclusions (cf. [1, 3]) that are isolated within coarse grid blocks. As a result, the coarse space contains all fine-scale functions with respect to slow variables within high-anisotropy channels. This can lead to a substantial dimension reduction; however, unlike to the isotropic high-conductivity case, the dimension of the coarse space can still be very large as discussed in the paper. Numerical results are presented. We also discuss techniques that allow us to use smaller dimensional coarse spaces at the expenses of solving several lower dimensional problems in the channels of high-anisotropy.

3 Problem Setting and Domain Decomposition Framework

Let $D \subset \mathbb{R}^2$ (or $\mathbb{R}^3$) be a polygonal domain which is the union of a disjoint polygonal subregions $\{D_i\}_{i=1}^N$. We seek $u \in H_0^1(D)$

$$a(u,v) := \int_D \kappa(x)\nabla u \cdot \nabla v dx = \int_D f v dx, \text{ where } \kappa(x) = \begin{pmatrix} \eta(x) & 0 \\ 0 & 1 \end{pmatrix}. \qquad (1)$$

Here $\eta(x)$ is a heterogeneous field with high contrast, $\eta(x) \geq 1$. More general cases where the direction of anisotropy can change continuously in space will be considered elsewhere. Next, we introduce some notations following [1].

We assume that $\{D_i\}_{i=1}^N$ form a quasiuniform triangulation of D and denote $H = \max_i \text{diam}(D_i)$. Let $\mathscr{T}^h$ be a fine triangulation which refine $\{D_i\}_{i=1}^N$. We denote by $V^h(D)$ the usual finite element discretization of piecewise linear continuous functions with respect to the fine triangulation $\mathscr{T}^h$. Denote also by $V_0^h(D)$ the subset of $V^h(D)$ with vanishing values on ∂D. Similar notations, $V^h(\Omega)$ and $V_0^h(\Omega)$, are used for subdomains $\Omega \subset D$.

The Galerkin finite element approximation of (1) is to find $u \in V_0^h(D)$ with $a(u,v) = \int_D fv$ for all $v \in V_0^h(D)$, or in matrix form

$$Au = b, \tag{2}$$

where for all $u, v \in V^h(D)$ (considered as vectors) we have $v^T Au = a(u,v)$ and $v^T b = \int_D fv$. We assume that κ is piecewise constant coefficient in $\mathscr{T}^h$ with value $\kappa = \kappa_e = (\eta_e, 0; 0, 1)$ on each fine triangulation element $e \in \mathscr{T}^h$.

We denote by $\{D_i'\}_{i=1}^N$ the overlapping decomposition obtained from the original nonoverlapping decomposition $\{D_i\}_{i=1}^N$ by enlarging each subdomain D_i to $D_i' = D_i \cup \{x \in D, \mathrm{dist}(x, D_i) < \delta_i\}$, $\quad i = 1, \ldots, N$, where dist is some distance function and let $\delta = \max_{1 \le i \le N} \delta_i$. Let $V_0^h(D_i')$ be the set of finite element functions with support in D_i'. We also denote by $R_i^T : V_0^h(D_i') \to V^h(D)$ the extension by zero operator.

We use a partition of unity $\{\xi_i\}_{i=1}^N$ subordinated to the covering $\{D_i'\}_{i=1}^N$ such that

$$\sum_{i=1}^N \xi_i = 1, \quad \xi_i \in V^h(D), \quad 0 \le \xi_i \le 1 \quad \text{and} \quad \mathrm{Supp}(\xi_i) \subset D_i', \ \ i = 1, \ldots, N, \tag{3}$$

where $\mathrm{Supp}(\xi_i)$ stands for the support of the function ξ_i. This partition of unity is used to truncate global functions to local conforming functions, an essential property in the construction of a stable splitting of the space.

Given a coarse triangulation $\mathscr{T}^H$, we introduce N_c coarse basis functions $\{\Phi_i\}_{i=1}^{N_c}$. We define the coarse space by $V_0^H = \mathrm{span}\{\Phi_i\}_{i=1}^{N_c}$, and the coarse matrix $A_0 = R_0 A R_0^T$ where $R_0^T = [\Phi_1, \ldots, \Phi_{N_c}]$. We use a two level additive preconditioner of the form

$$B^{-1} = R_0^T A_0^{-1} R_0 + \sum_{i=1}^N R_i^T A_i^{-1} R_i = R_0^T A_0^{-1} R_0 + B_{1L}^{-1}, \tag{4}$$

where $B_{1L}^{-1} = \sum_{i=1}^N R_i^T A_i^{-1} R_i$ and the local matrices are defined by $vA_i w = a(v,w)$ for all $v, w \in V_0^h(D_i')$, $i = 1, \ldots, N$ (see [5]).

We denote by $\{y_i\}_{i=1}^{N_v}$ the vertices of the coarse mesh $\mathscr{T}^H$ and define

$$\omega_i = \bigcup \{K \in \mathscr{T}^H; \ \ y_i \in \overline{K}\}, \ \ \omega_K = \bigcup \{\omega_j; \ \ y_j \in \overline{K}\}. \tag{5}$$

Additionally, we use a partition of unity $\{\chi_i\}_{i=1}^{N_v}$ subordinated to the covering $\{\omega_i\}_i^{N_v}$ such that

$$\sum_{i=1}^{N_v} \chi_i = 1, \quad \chi_i \in V^h(D), \quad 0 \le \chi_i \le 1 \quad \text{and} \quad \mathrm{Supp}(\chi_i) \subset \omega_i, i = 1, \ldots, N_v. \tag{6}$$

4 Coarse Space Construction and Dimension Reduction

In this section we define a local spectral multiscale coarse space using eigenvectors of high-anisotropy eigenvalue problems. First we introduce the notation for eigenvalue

problems following [1]. For $i = 1,\dots,N_v$, define the matrix A^{ω_i} and the *modified mass matrix* of same dimension M^{ω_i} by

$$v^T A^{\omega_i} w = \int_{\omega_i} \kappa \nabla v \cdot \nabla w dx \ \text{ and } \ v^T M^{\omega_i} w = \int_{\omega_i} \widetilde{\kappa} v w dx \ \ \forall v, w \in \widetilde{V}^h(\omega_i), \qquad (7)$$

where $\widetilde{V}^h(\omega_i) = \{v \in V^h(\omega_i) : v = 0 \text{ on } \partial\omega_i \cap \partial D\}$. Here $\widetilde{\kappa}$ is an scalar weight derived from the high-anisotropy coefficient matrix $\kappa = [\kappa_{ij}]$ and contains the relevant information we need for the construction of the coarse basis functions. Several possible choices for $\widetilde{\kappa}$ can be considered. Here $\widetilde{\kappa}$ is defined by

$$\widetilde{\kappa} = \max\left\{ \sum_{i=1}^{N} \kappa \nabla \xi_i \cdot \nabla \xi_i, \sum_{j=1}^{N_v} \kappa \nabla \chi_j \cdot \nabla \chi_j \right\}, \qquad (8)$$

where $\{\xi_j\}_{j=1}^N$ and $\{\chi_i\}_{i=1}^{N_v}$ are the partition of unity introduced in (3) and (6), respectively. From now on, we assume that the overlapping decomposition is constructed from the coarse mesh and then $\xi_i = \chi_i$ and $D_i' = \omega_i$ for all $i = 1,\dots,N = N_v$, and $\delta \asymp H$. We consider the finite dimensional symmetric eigenvalue problems $A^{\omega_i}\psi = \widetilde{\lambda} M^{\omega_i}\psi$, with A^{ω_i} and M^{ω_i} defined by (7) and (8), $i = 1,\dots,N$. Denote its eigenvalues and eigenvectors by $\{\widetilde{\lambda}_\ell^{\omega_i}\}$ and $\{\psi_\ell^{\omega_i}\}$, respectively. Note that the eigenvectors $\{\psi_\ell^{\omega_i}\}$ form an orthonormal basis of $\widetilde{V}^h(\omega_i)$ with respect to the M^{ω_i} inner product. Assume that $\widetilde{\lambda}_1^{\omega_i} \le \widetilde{\lambda}_2^{\omega_i} \le \cdots \le \widetilde{\lambda}_\ell^{\omega_i} \le \dots$, and note that $\widetilde{\lambda}_1^{\omega_i} = 0$ for all interior subdomains. In particular, $\psi_\ell^{\omega_i}$ denotes the ℓ-th eigenvector of the matrix associated to the neighborhood of y_i, $i = 1,\dots,N_v$.

Let $\{\chi_i\}_{i=1}^{N_v}$ be a partition of unity (3). Define the coarse basis functions

$$\Phi_{i,\ell} = I^h(\chi_i \psi_\ell^{\omega_i}) \quad \text{for } 1 \le \ell \le L_i \text{ and } 1 \le i \le N_v, \qquad (9)$$

where I^h is the fine-scale nodal value interpolation and L_i is an integer number for each $i = 1,\dots,N_v$. Denote by V_0^H the *spectral multiscale* space

$$V_0^H = \text{span}\{\Phi_{i,\ell} : 1 \le \ell \le L_i \text{ and } 1 \le i \le N_v\}. \qquad (10)$$

The idea is to use only eigenvectors of contrast dependent eigenvalues. Next, we discuss how the choice of $\widetilde{\kappa}$ affects the eigenvalues. If we choose χ_i to be piecewise linear functions on the coarse grid, then, it is easy to see that we have $\widetilde{\kappa}(x_1,x_2) = \sum_i \eta(x_1,x_2)|\partial_{x_1}\chi_i(x_1,x_2)|^2 + |\partial_{x_2}\chi_i(x_1,x_2)|^2$ and $\widetilde{\kappa}$ will have similar behavior as $\eta(x)$. In this case, one can show that the number of small eigenvalues is the same as the fine degrees of freedom in the form of discrete functions that depend on x_2 within high-anisotropy inclusions and channels. Indeed, if we consider the associated Rayleigh quotient, $R(v) = \frac{v^T A^{\omega_i} w}{v^T M^{\omega_i} w}$, we have

$$R(v) = \frac{\int_{\omega_i} \kappa \nabla v \cdot \nabla v}{\int_{\omega_i} \widetilde{\kappa} v^2} = \frac{\int_{\omega_i} \eta(x_1,x_2)|\partial_{x_1} v(x_1,x_2)|^2 + |\partial_{x_2} v(x_1,x_2)|^2}{\int_{\omega_i} \left(\sum_i \eta(x_1,x_2)|\partial_{x_1}\chi_i(x_1,x_2)|^2 + |\partial_{x_2}\chi_i(x_1,x_2)|^2\right) v(x_1,x_2)^2}.$$

Then, for functions that depends only on x_2 inside the region R where η is high, the numerator reduces to $\int_{\omega_i \setminus R} \left(|\partial_{x_1} v(x_1,x_2)|^2 + |\partial_{x_2} v(x_1,x_2)|^2\right) + \int_R |\partial_{x_2} v(x_1,x_2)|^2$

(which is independent of the high value of $\eta(x)$ in R) and the quotient will go to zero as the value of η in R goes to infinity. Including all fine grid functions of x_2 into the coarse space can lead to a high dimensional coarse spaces. Note that the dimension of the coarse space will be much higher than the case with scalar coefficient κ where the number of small eigenvalues is equal to the number of isolated inclusions and channels within a coarse block; see [1, 3]. To reduce the dimension of the coarse space, we propose the use of multiscale basis functions.

We are interested in partition of unity functions that can reduce the number of degrees of freedom associated with isolated high-anisotropy inclusions. This can be achieved by minimizing high-conductivity components for the scalar function $\widetilde{\kappa}$. In particular, by choosing multiscale finite element basis functions or energy minimizing basis functions (e.g., [6]), we can eliminate all isolated high-conductivity inclusions. This can be observed in our numerical experiments. We recall the definition of the "standard" multiscale finite element basis functions that coincide with (the piecewise linear functions on the coarse grid) χ_i^0 on the boundaries of the coarse partition. They are denoted by χ_i^{ms} and satisfy:

$$-\operatorname{div}(\kappa\nabla\chi_i^{ms}) = 0 \ \text{ in } K \in \omega_i, \quad \chi_i^{ms} = \chi_i^0 \ \text{ in } \partial K, \ \ \forall\, K \in \omega_i, \tag{11}$$

where K is a coarse grid block within ω_i, see [2] for more details and more general multiscale basis functions constructions. In Fig. 1, we depict $\eta(x)$ (left picture) and $\widetilde{\kappa}$ (right picture) using multiscale basis functions on the coarse grid. One can observe that isolated inclusions are removed in $\widetilde{\kappa}$. The coarse space contains functions depending only on x_2 within long channels. The situation is more complicated if high-anisotropy regions form complex channel patterns. For example, if high-anisotropy region is vertical for the coefficients considered in our numerical example, then initial multiscale spaces can represent them and no additional degrees are needed. More complex channel shapes will be studied elsewhere.

We note that for the proposed methods, in each ω_i, $i = 1, \ldots, N_v$, we only need to specify the number of eigenvectors L_i based on the quantities $\{1/\widetilde{\lambda}_l^{\omega_i}\}$. These eigenvectors are used to construct the coarse space. In practice, one only needs to compute the first L_i eigenvalues. Hierarchical approximation with several triangulations can also be considered for the eigenvalues and eigenvectors.

Weighted L^2 approximation and weighted H^1 stability properties of the coarse space V_0^H in (10) hold (as in [1, 3]). In order to describe better these properties of V_0^H, we need to introduce a relevant interpolation operator. Given $v \in V^h(\omega_i)$, set

$$I_{L_i}^{\omega_i} v = \sum_{\ell=1}^{L_i} \left(\int_{\omega_i} \widetilde{\kappa} v \psi_\ell^{\omega_i} dx \right) \psi_\ell^{\omega_i}, \quad i = 1, \ldots, N_v, \tag{12}$$

and define the coarse interpolation $I_0 : V^h(D) \to V_0^H$ by

$$I_0 v = \sum_{i=1}^{N_v} \sum_{\ell=1}^{L_i} \left(\int_{\omega_i} \widetilde{\kappa} v \psi_\ell^{\omega_i} dx \right) I^h(\chi_i \psi_\ell^{\omega_i}) = \sum_{i=1}^{N_v} I^h \left(\chi_i (I_{L_i}^{\omega_i} v) \right), \tag{13}$$

where I^h is the fine-scale nodal value interpolation.

Lemma 1. *For each coarse element K we have*

- $\int_K \widetilde{\kappa}(v - I_0 v)^2 \preceq \widetilde{\lambda}_{K,L+1}^{-1} \int_{\omega_K} \kappa \nabla v \cdot \nabla v dx$
- $\int_K \kappa \nabla I_0 v \cdot \nabla I_0 v dx \preceq \max\{1, \widetilde{\lambda}_{K,L+1}^{-1}\} \int_{\omega_K} \kappa \nabla v \cdot \nabla v dx,$

where $\widetilde{\lambda}_{K,L+1} = \min_{y_i \in K} \widetilde{\lambda}_{L_i+1}^{\omega_i}$ and ω_K is defined in (5).

Using Lemma 1, we can estimate the condition number of the preconditioned operator $B^{-1}A$ with B^{-1} defined in (4) using the coarse space V_0^H in (10). Following [1, 3], one has the following result.

Theorem 1. *The condition number, $cond(B^{-1}A)$, of the preconditioned operator $B^{-1}A$ with B^{-1} defined in (4) satisfies*

$$cond(B^{-1}A) \preceq 1 + \widetilde{\lambda}_{L+1}^{-1}, \quad \text{where} \quad \widetilde{\lambda}_{L+1} = \min_{1 \le i \le N_v} \widetilde{\lambda}_{L_i+1}^{\omega_i}.$$

Recall that we assumed $\xi_i = \chi_i$, $i = 1, \ldots, N = N_v$. It can be easily shown that if we choose L_i as the number of contrast dependent eigenvalues, then $\widetilde{\lambda}_{L+1}$ scales as $O(1)$, i.e., independent of the contrast. The dependency of the condition number on δ and H is controlled by the partition of unity $\{\chi_i\}$. The condition number is independent of h and it is, in the general case of different partitions of unity, $\{\chi_i\}$ and $\{\xi_i\}$, of order $O(H^2/\delta^2)$, see [3].

5 Numerical Results

In this section, we show representative $2D$ numerical results for the additive preconditioner (4) with the local spectral multiscale coarse space defined in (10). We take $D = [0,1] \times [0,1]$ that is divided into 10×10 equal square coarse blocks to construct the coarse mesh. Inside each coarse block we use a fine-scale triangulation where triangular elements constructed from 10×10 squares are used.

We test our approach on a permeability field that contains inclusions and channels on a background of conductivity one (see the left picture of Fig. 1 for $\eta(x)$ in (1)). We use multiscale finite element basis functions as the initial partition of unity. From the right picture of Fig. 1 we see that the modified weight $\widetilde{\kappa}$ does not contain any isolated inclusions and only contains long high-anisotropy channels connecting boundaries of coarse-grid blocks. This is automatically achieved from the choice of the partition of unity functions. There are fewer small (asymptotically vanishing) eigenvalues when local eigenvalue problem is solved with the modified weight $\widetilde{\kappa}$. Thus, a good choice of partition of unity functions χ_i in (8) will ensure fewer new multiscale basis functions needed to achieve an optimal convergence with respect to the contrast. Numerical results are presented in Table 1. We observe that using the proposed coarse spaces, the number of iterations is independent of contrast. In Table 1 we also show the dimension of the coarse spaces. The dimension of the local spectral coarse space is smaller if we use $\widetilde{\kappa}$ in (10) with multiscale basis functions instead of piecewise linear basis functions.

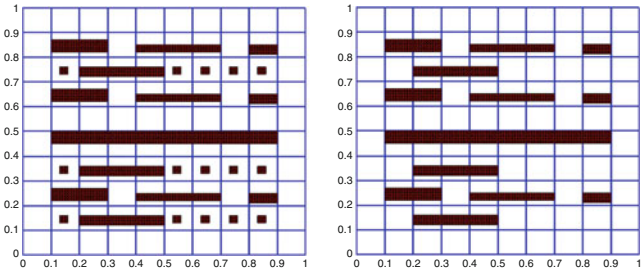

Fig. 1. *Left*: Coarse mesh and coefficient (we plot $\eta(x) = 10^6$ and recall that $\eta(x) = 1$ elsewhere). *Right*: Coefficient $\widetilde{\kappa}$ in (8) using multiscale basis functions (we plot $\widetilde{\kappa}(x) \geq 10^6$). See Table 1

η	LIN	MS	EMF	LSM (bilin. χ_i)	LSM (MS χ_i)	
10^3	113(1.48e+2)	122(1.51e+2)	115(1.81e+2)	53(23.21)	55(26.9)	t1.1 t1.2
10^4	257(1.35e+3)	258(1.28e+3)	231(9.70e+2)	41(53.63)	28(5.82)	t1.3
10^5	435(1.34e+4)	483(1.26e+4)	416(9.64e+3)	28(5.642)	29(6.02)	t1.4
10^6	627(1.34e+5)	709(1.27e+5)	599(9.63e+4)	30(5.753)	29(6.04)	t1.5
Dim	81=0.79%	81=0.79%	81=0.79%	732=7.19%	497=4.87%	t1.6

Table 1. Number of iterations and estimated condition number for the PCG and various values of η with the coefficient depicted in Figure 1. We set the tolerance to $1e-10$, $H = 1/10$, $h = 1/100$, and $\dim(V_h) = 10201$. The notation MS stands for the (linear boundary condition) multiscale (MS) coarse space, EMF is the energy minimizing coarse space, see e.g., [6], and LSM is the local spectral multiscale coarse space defined in (10). We select the first L eigenvalues such that $\tilde{\lambda}_L - \tilde{\lambda}_{L-1} > 0.05$ (which is and easy way to select the small eigenvalues- in this example, the value 0.05 was chose by trial-and-error).

6 Discussion on Coarse Space Dimension Reduction

Now we discuss approaches to avoid the use of high-dimensional coarse spaces without sacrificing the efficiency of the preconditioner at the expense of solving problems in high-anisotropy channels. As was observed in the presented numerical tests, the strongly anisotropic channels cause a substantial increase of the size of the coarse space and the complexity of the method. To avoid this, we can replace the coarse solve $R_0^T A_0^{-1} R_0$ in (4) by $R_0^T \widetilde{A}_0^{-1} R_0 + R_{an}^T A_{an}^{-1} R_{an}$. Here the matrix $\widetilde{A}_0$ is a small dimensional coarse matrix. The matrix A_{an} is acting on the fine-mesh degrees restricted to subdomain of high-anisotropy channels Ω_{an}. It is based on the original matrix A and is constructed locally (element-by-element) by preserving the strongest links (off-diagonal entries) of the element stiffness matrices in the channels. To illustrate this idea, which was developed in [4] for Crouzeix-Raviart elements, we write an element stiffness matrix A_e for $e \subset \Omega_{an}$: $A_e = [b_e + c_e,\ -c_e,\ -b_e; -c_e,\ a_e + c_e,\ -a_e; -b_e,\ -a_e,\ a_e + b_e]$, where $|a_e| \leq b_e \leq c_e$. Then the matrix A_{an} is defined as assembly of the matrices $B_e = [c_e,\ -c_e,\ 0; -c_e,\ c_e,\ 0; 0,\ 0,\ 0]$, $e \subset \Omega_{an}$. It is easy

to see that A_{an} is a stiffness matrix corresponding to a diffusion problem defined on a carcass of piecewise linear lines in Ω_{an} following the directions of dominating anisotropy.

In the case of apparent dominant anisotropy direction (i.e., when A_{an} is block diagonal with tridiagonal blocks), inverting A_{an} will involve solving block-diagonal problems with tridiagonal blocks (in 2-D only). In this case optimal complexity is achieved by using a sparse direct solver. In general, one may consider including some of the degrees of freedom associated with high-anisotropy regions into the coarse space while using A_{an}^{-1} to handle the others. Another possibility is to use an auxiliary space of Crouzeix-Raviart elements combined with the technique from [4]. These issues will be studied in our subsequent work.

Acknowledgments The work of all authors has been partially supported by award KUS-C1-016-04, made by King Abdullah University of Science and Technology (KAUST). The work of RL has been supported in part by the US NSF Grant DMS-1016525. The work of SM was partially supported by the Bulgarian NSF Grant DO 02-147/08. The work of YE has been supported by the DOE and NSF (DMS 0934837, DMS 0902552, and DMS 0811180).

Bibliography

[1] Y. Efendiev and J. Galvis. A domain decomposition preconditioner for multiscale high-contrast problems. In Y. Huang, R. Kornhuber, O. Widlund, and J. Xu, editors, *Domain Decomposition Methods in Science and Engineering XIX*, volume 78 of *Lecture Notes in Computational Science and Engineering*, pages 189–196. Springer, 2011.

[2] Yalchin Efendiev and Thomas Y. Hou. *Multiscale finite element methods. Theory and applications*, volume 4 of *Surveys and Tutorials in the Applied Mathematical Sciences*. Springer, New York, 2009.

[3] Juan Galvis and Yalchin Efendiev. Domain decomposition preconditioners for multiscale flows in high contrast media: reduced dimension coarse spaces. *Multiscale Model. Simul.*, 8(5):1621–1644, 2010.

[4] J. Kraus and S. Margenov. *Robust Algebraic Multilevel Methods and Algorithms*, volume 5 of *Radon Series on Comput. Appl. Math.* de Gruyter, 2009.

[5] Andrea Toselli and Olof Widlund. *Domain decomposition methods—algorithms and theory*, volume 34 of *Springer Series in Computational Mathematics*. Springer-Verlag, Berlin, 2005.

[6] Jinchao Xu and Ludmil Zikatanov. On an energy minimizing basis for algebraic multigrid methods. *Comput. Vis. Sci.*, 7(3-4):121–127, 2004.